doi:10.1016/j.jmb.2009.08.045 J. Mol. Biol. (2009) 393, 909–919

JMB

Available online at www.sciencedirect.com

ScienceDirect

ELSEVIER

# Illuminating Solution Responses of a LOV Domain Protein with Photocoupled Small-Angle X-Ray Scattering

**Jessica S. Lamb[1], Brian D. Zoltowski[2], Suzette A. Pabit[1], Li Li[1], Brian R. Crane[2]* and Lois Pollack[1]***

[1]*School of Applied and Engineering Physics, Cornell University, Ithaca, NY 14853, USA*

[2]*Department of Chemistry and Chemical Biology, Cornell University, Ithaca, NY 14853, USA*

*Received 28 May 2009; received in revised form 14 August 2009; accepted 18 August 2009*
Available online 25 August 2009

The PAS–LOV domain is a signal-transducing component found in a large variety of proteins that is responsible for sensing different stimuli such as *l*ight, *o*xygen, and *v*oltage. The LOV protein VVD regulates blue light responses in the filamentous fungi *Neurospora crassa*. Using photocoupled, time-resolved small-angle X-ray scattering, we extract the solution protein structure in both dark-adapted and light-activated states. Two distinct dark-adapted conformations are detected in the wild-type protein: a compact structure that corresponds to the crystal structure of the dark-state monomer as well as an extended structure that is well modeled by introducing conformational disorder at the N-terminus of the protein. These conformations are accentuated in carefully selected variants, in which a key residue for propagating structural transitions, Cys71, has been mutated or oxidized. Despite different dark-state conformations, all proteins form a common dimer in response to illumination. Taken together, these data support a reaction scheme that describes the mechanism for light-induced dimerization of VVD. Envelope reconstructions of the transient light-state dimer reveal structures that are best described by a parallel arrangement of subunits that have significantly changed conformation compared to the crystal structure.



*Keywords:* LOV domain proteins; blue light activated proteins; VVD; photocoupled small-angle X-ray scattering

***Edited by I. Wilson***

## Introduction

Biological signal transduction systems rely on the ability of intracellular proteins to alter their structures and patterns of association in response to external stimuli. The PAS (Per Arnt Sim) domain is a broadly distributed protein module often found as a component of signaling networks.[1] PAS domains, either in isolation or as part of a multidomain protein, regulate many different cellular processes, including kinase activity, gene transcription, and channel function.[2]

LOV domain proteins (for *l*ight, *o*xygen, and *v*oltage sensing), which form a subclass of the PAS superfamily, bind cofactors that react chemically to sense changes in ligand concentration, illumination, and redox state. Structural dynamics in LOV proteins have been well characterized in plant phototropins and related phototropin-like photoreceptors,[3–6] where blue light triggers the formation of a cysteinyl flavin C4a adduct, which then relays conformational changes to variable N- or C-terminal extensions of the PAS core.[7,8] The consequences of such processes have been explored in several systems. For example, plant phototropins undergo autophosphorylation to regulate growth,[9,10] fungal white collar 1 (WC-1) activates gene expression,[11,12] and bacterial YtvA modulates stress responses.[13] In all of these cases, the mechanisms that link photo-adduct formation to downstream changes in molecular reactivity are not well understood.

**Corresponding authors.* E-mail addresses: lp26@cornell.edu; bc69@cornell.edu.

Present addresses: J. S. Lamb, NIDCD, National Institutes of Health, Bethesda, MD 20892, USA; B. D. Zoltowski, UT Southwestern Medical Center, Dallas, TX 75390, USA.

Abbreviations used: PAS, Per Arnt Sim; WC-1, fungal white collar 1; SAXS, small-angle X-ray scattering; CHESS, Cornell High Energy Synchrotron Source.

Here, we investigate the initial steps in the light-activated response of the fungal PAS–LOV photosensor Vivid (VVD) by monitoring global changes in protein structure triggered by the absorption of a single photon. Vivid is involved in adaptation to blue light responses such as carotenoid production and gating of the circadian clock in the filamentous fungus *Neurospora crassa*.[14,15] VVD may also sense intracellular oxidants, such as superoxide; however, the underlying molecular processes have yet to be explored.[16] Spectroscopic and crystallographic studies[15,17] of VVD revealed that cysteine 108 forms an adduct in response to blue light. The crystallographic structure of the light-activated state (Fig. 1) further showed how adduct formation couples to flavin N5 protonation. N5 protonation in turn drives hydrogen-bonding rearrangements that alter the conformation of the Ncap, which is composed of N-terminal structural elements that pack against the PAS β-core. In VVD, the Ncap consists of an extended stretch of polypeptide that begins near the adenosine moiety of the flavin, an α-helix (aα), a short β-strand (bβ), and a short hinge that connects the rest of the Ncap to the PAS core through the key switching residue Cys71.[17] In the crystal, light causes a shift in bβ, but in solution, the current data suggest that a more dramatic structural response in the Ncap ultimately leads to dimerization.[17–19] It is currently not clear how the conformational changes observed in the crystal structure of the light state facilitate dimerization.

PAS:PAS dimerization is not unique to VVD and plays a significant role in signaling by other PAS domains.[10,11] Whereas stable PAS dimers have been structurally characterized,[20–23] their solution dynamics and *in vivo* relevance remain to be established. Recently, transient gradient methods have demonstrated that phototropin LOV domains can also form light-induced dimers,[24] but again, their role in the context of the full-length proteins is largely unexplored. Solution small-angle X-ray scattering (SAXS) reports global structural characteristics of macromolecules and is ideal for studying large conformational changes, including association processes.[25]

We have previously employed photocoupled SAXS to demonstrate dimerization of the VVD light state on a rapid time scale. The biologically inactive C71S variant was also shown to be incapable of dimerization.[17] Here, we further apply SAXS to resolve important structural characteristics of the light- and dark-adapted states of two VVD proteins: VVD-36, an N-terminal truncation of wt VVD with increased stability and solubility,[17,18] and VVD-36: C71V:C183S, which forms a higher-affinity light-state dimer due to the residue substitution at position 71.[18] We employ a flow cell that enables time-resolved measurements as rapidly as 20 ms after photoexcitation and, furthermore, mitigates radiation damage from X-rays, which can confound the interpretation of SAXS data. Two distinct dark-state structures that both lead to a single dimer were discovered and analyzed. By reconstructing the SAXS data into low-resolution molecular envelopes, we show that dimerization indeed requires substantial conformational change in the VVD monomer.[18] Analysis of these structures leads us to propose a mechanism for dimerization of VVD. A similar conformational gate may regulate transient dimerization in other LOV/PAS systems.

## Results

The long-term goal of this work is to identify the mechanism underlying light-induced conformational changes of VVD. To achieve this goal, we mea-

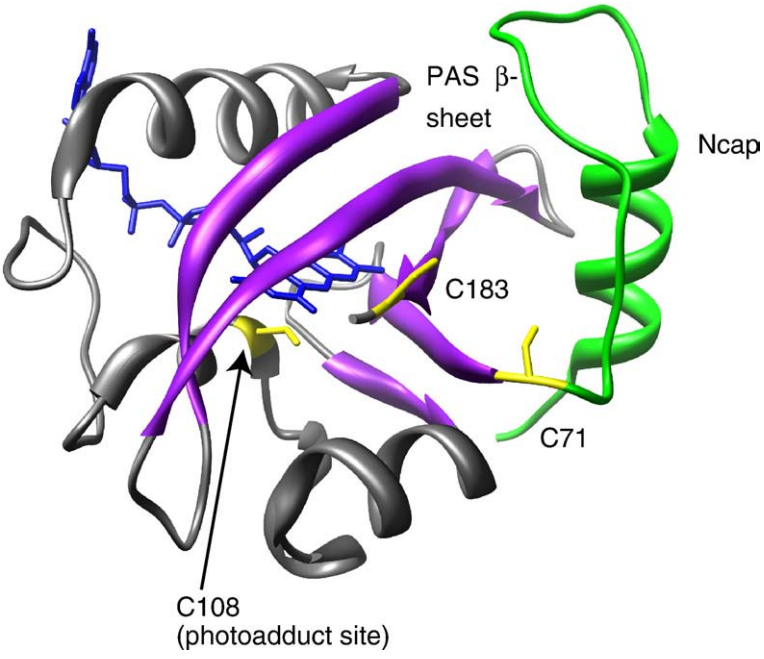


**Fig. 1.** Crystal structure of VVD (Protein Data Bank code: 2PDR). The Ncap is shown in green, the β-core is shown in purple, and the adduct forming flavin is shown in blue. All relevant Cys residues are shown in yellow.

sured the structure of VVD in both dark- and light-adapted states, using a SAXS compatible flow cell. Previous studies indicate that VVD dimerizes after exposure to light but did not reveal the solution structure of, or the mechanism for, dimer formation.[18,19] Here, we extract details about the solution protein structure in both dark and light states and use this information to propose a mechanism that drives this transition.

To enable such biophysical characterization, we employ variants of full-length VVD that increase protein solubility, stability, and resistance to oxidation. Removal of 36 residues from the N-terminus of VVD that are variable compared to related LOV domains increases the protein's stability and ability to undergo multiple photocycles.[17,18] Otherwise, VVD-36 shows similar light-dependent dimerization as the full-length protein.[17] A point mutation near the C-terminus (C183S) greatly reduces the tendency to form intermolecular disulfide bonds at high concentrations and otherwise deactivate in the presence of oxidants. C183S alone has no known effects on VVD spectral characteristics or dimerization kinetics.

## Two VVD dark-state conformations: Extended and compact

SAXS data were collected on samples from numerous preparations of protein. A given batch of dark-adapted VVD-36 displays one of two distinct conformational ensembles, shown in Fig. 2. The scattering profile of one of these ensembles exactly matches profiles generated from the crystal structure,[17] while the other suggests a structure with a larger spatial extent. Comparison of radius of gyration reveals little difference, with the former data set yielding a value of $R_g = 18.1 \pm 1.1$ Å and the latter yielding $R_g = 18.8 \pm 0.6$ Å. To elucidate differences between the two states, we compared distance distribution functions [$P(r)$] computed from the latter structure with those computed from the former structure, using the 2PD7 coordinates to minimize the noise (Fig. 2). This analysis emphasizes the spatial dimensions of the protein and requires input of the maximum molecular dimension, $D_{max}$, to accurately reproduce the scattering data. The $D_{max}$ value required to reproduce scattering from the larger structure exceeds that required for the crystal structure. Because of its larger spatial extent, we refer to the first, extended state as $Dark_{EXT}$, while the more compact state that agrees with the crystal structure will be referred to as $Dark_{COMP}$.

To associate a structural feature with this extension, we turn to results from other biochemical studies of VVD-36. Recent crystal structures display an alternate conformation of the first eight N-terminal residues.[18] In addition, cross-linking studies of the light-activated conformation of VVD indicate that the N-terminal α-helix may reorient to form the light-state dimer.[18] The Ncap region is the site of the largest rearrangements upon light excitation of the crystallized protein. Taken together, this evidence suggests that reorganization of the N-terminus accounts for the difference between the $Dark_{EXT}$ state and the conformation in the crystal.

In order to assess the length of the N-terminus polypeptide that must rearrange to describe the SAXS data, we conducted computational studies with EOM.[26] This program generates an ensemble of unfolded or partly unfolded structures from an amino acid sequence and, with a genetic algorithm, searches for a subset of these that combine to match the experimental data. This analysis was performed six times, including selectively longer portions of the Ncap in the unfolded ensemble (Fig. 3). Notably, extension of only the eight terminal peptides, which form alternate conformations in some crystal structures,[18] is insufficient to describe the data. At a minimum, the N-terminal peptide chain and the N-terminal α-helix must be displaced to obtain good agreement between the calculated and measured SAXS profiles.

Flexibility in other regions of the molecule may contribute to the extended structure. For example, there are indications from thermal factors in the

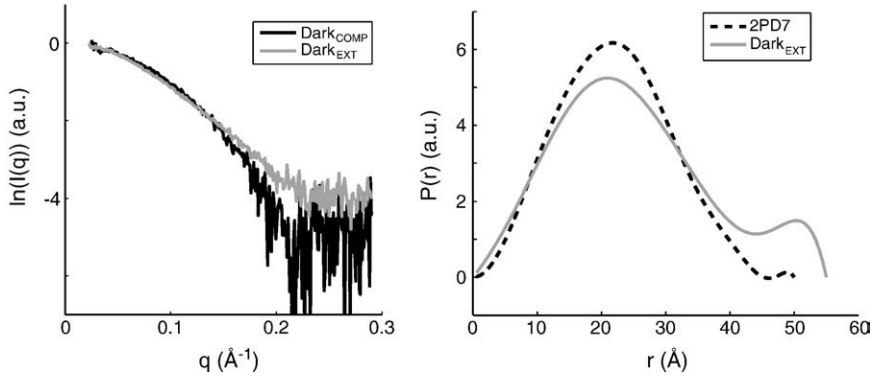


**Fig. 2.** Comparison of scattering profiles from two dark states, $Dark_{COMP}$ and $Dark_{EXT}$. The left panel compares scattering profiles from the two distinct dark states of VVD-36: $Dark_{COMP}$ and $Dark_{EXT}$. The right panel shows $P(r)$ profiles computed from the $Dark_{EXT}$ scattering data and from scattering profiles generated from (a monomer within) the 2PD7 crystal structure. The $Dark_{EXT}$ conformation has a larger apparent maximum dimension and the corresponding $P(r)$ curve peaks at a slightly higher value of $r$, indicating more extended molecules within the ensemble.

crystal structures that the loop regions surrounding the adenosine moiety of FAD, as well as the adenosine itself, are quite dynamic.[17,18] Thus, we must allow that the conformational disorder required to describe the SAXS data does not necessarily involve the entire Ncap if other regions of the protein are also involved. Nonetheless, a substantial number of residues change their conformational state in going from the compact to the extended form of the protein, and these changes likely involve the N-terminus.

### Conversion between the dark states

Each state appeared uniquely represented within a given batch of protein, and no interconversion was measured on a time scale of 24 h, suggesting that both correspond to stable conformational states of the protein. After extensive experimentation, we have found that the emergence of $Dark_{COMP}$ correlates with the age and treatment of the protein. The $Dark_{EXT}$ state was consistently found with either freshly prepared protein or protein that was treated with the reducing agent DTT. In fact, a sample of $Dark_{COMP}$ could be converted to $Dark_{EXT}$ on incubation with DTT. Protein that was left at 4 °C overnight or repurified in the absence of DTT consistently showed the $Dark_{COMP}$ conformation. Thus, we suspect that oxidation plays an important role in formation of $Dark_{COMP}$. It should also be noted that degradation at the N-terminus of VVD-36 can prevent dimerization,[18] and in some long experiments, minor amounts of N-terminal degradation were observed. However, samples clearly in the $Dark_{COMP}$ state showed no evidence of proteolysis.

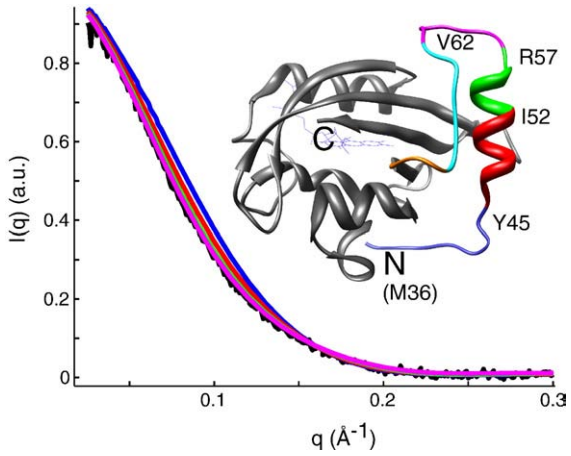


**Fig. 3.** Results of the EOM analysis. The smooth curves are scattering profiles computed from an ensemble of partially extended molecules, beginning with the 3D72 crystal structure (inset). In these models, varying lengths of the amino acid chain, denoted by different colors, are allowed to be flexible. To generate the curves shown here, 10, 17, 22, and 28 residues are displaced; agreement with the measured curve improves as more residues become flexible. Scattering curves generated from the first two ensembles (10 or 17 residues flexible, blue and red curves) do not fit the data well. In contrast, extending residues 36–58, which includes the entire N-terminal α-helix, produces a reasonable fit. The match to the data is further improved if the loop that connects the α-helix with the LOV domain is made flexible.

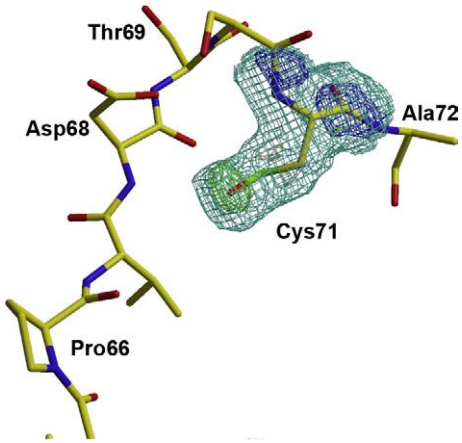


**Fig. 4.** Oxidation of VVD at Cys71 to a sulfenic acid. $F_o-F_c$ maps (at 2.3 Å resolution) calculated from structures containing a Cys at position 71 instead of the sulfenic acid clearly show the presence of the additional oxygen atom (contoured at 3 σ, green). $2F_o-F_c$ density is contoured at 1 σ (cyan) and 2 σ (blue).

### Oxidation at Cys71 alters protein structure

We have observed in many contexts that both passive and promoted oxidation affect the extent to which VVD undergoes light-induced dimerization (Supplementary Fig. 1). Passive oxidation correlates with the length of time the protein resides in oxygenated, aqueous buffer. To investigate whether oxidation may underlie the difference between the two forms of dark-state VVD, crystal structures were obtained from VVD protein that had been aged several days in oxygenated buffer. These structures show additional electron density at Cys71 indicative of oxidation of this key residue to sulfenic acid (-S-OH) (Fig. 4). The 2.3-Å-resolution electron density is fit well by addition of a single oxygen atom and, when modeled as such, generates no difference electron density peaks. Furthermore, the CH2-S-O (H) bond angle agrees well with that expected for sulfenic acid. The data presented above and in previous studies demonstrate that Cys71 participates in a conformational switch that is essential for dimerization and protein function.[17] Thus, we believe oxidation of this important residue to be at least partly responsible for generating dark-state samples with different conformational properties.

### Light activation of VVD

Within 300 ms of light excitation, scattering profiles from VVD-36 in both compact and extended forms indicate dimerization. Figure 5 shows the dramatic increase in scattering intensity at low $q$ for both molecules that reflects dimerization. Follow-

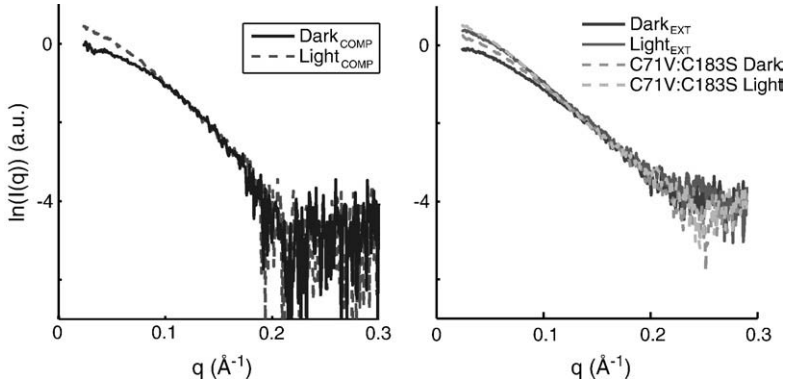


**Fig. 5.** Comparison of dark- and light-excited scattering data. The left panel compares scattering profiles from the Dark$_{COMP}$ state of VVD-36 in the dark-adapted (continuous line) and light-activated (broken line) states. The increase at the lowest scattering angles indicates dimerization of the protein following light exposure. The right panel shows a similar effect in scattering profiles of VVD-36 in the Dark$_{EXT}$ state (dark-adapted state: darker continuous line, light-activated state: lighter continuous line). Scattering profiles of the VVD variant C71V:C183S are shown as broken lines in the right panel. The scattering profiles of this variant match those of the Dark$_{EXT}$ state at mid to high $q$. The enhanced low-angle scattering of this variant relative to the Dark$_{EXT}$ conformation suggests the presence of dimers in the dark-adapted state of the variant (dark, broken line). Light excitation further increases the dimer fraction of the variant (light, broken line).

ing standard Guinier analysis, the zero-angle intensity is measured and found to increase by factors of 1.76±0.07 and 1.64±0.04 with Dark$_{COMP}$ and Dark$_{EXT}$ as respective initial states, less than the factor of 2 expected for complete conversion to dimers. Spectroscopic measurements reveal that only ~70% of the population forms the photo adduct under these solution and excitation conditions. Thus, the scattering collected from the light-excited states is a mixture of at least two states for each curve: light-activated dimers and dark-state monomers. The light-excited SAXS profiles preserve the shape observed in the high $q$ range of the dark-state monomer profiles, either reflecting different light-state dimers originating from the distinct initial states or resulting from residual monomers in the ensembles. The more detailed mathematical analysis of the data, presented later, clearly favors the latter scenario.

## An activated VVD variant: Extended and pretriggered in the dark state

The importance of the Cys71 residue to VVD conformation has already been discussed. Variation of this residue can profoundly impact the protein's response to light; for example, the C71S variant forms a cysteinyl–flavin adduct but is biologically inactive.[17] Here, we studied a different variant, C71V, which appears biased towards the light-state conformation, even in the dark-adapted state.[18] Previous crystallographic studies show that the side chain of Cys71 rotates out from a buried position upon VVD light excitation. This movement leads to functionally relevant conformational change at the N-terminus of the protein.[17] Crystal structures of VVD C71V show that Val71 can simultaneously occupy both Cys71 rotamer positions observed in native light- and dark-state structures. Thus, Val71 predisposes VVD to the light-state conformation even in the absence of light.

Following light excitation, data acquired on the C71V variant display a similar change in $I(0)$, although the dark-adapted ensemble of this variant appears heterogeneous. Interestingly, the shape of the high $q$ scattering from the Dark$_{EXT}$ and the C71V variant is in good agreement. When the intensities of these scattering profiles are scaled to match at high $q$, the low $q$ scattering from the variant exceeds that of the wild type and approaches that from the light state (Fig. 5). This increase suggests that the C71V variant dimerizes to some extent without light excitation (see Supplementary Fig. 2). We deduce that the variant monomer is predisposed to a conformation competent for dimerization because the Val side chain partly mimics the light-state conformation of Cys71.

Although dimerization is initiated in the dark state for the C71V variant, it is incomplete. Following illumination, $I(0)$ increases by an additional factor of 1.38±0.03, indicating further dimerization. This is consistent with previous work showing that light-induced dimers of C71V variants have dissociation constants in the nanometer range, as opposed to ~2–15 μM for VVD-36.[18] Thus, while the mutation of Cys71 to Val appears crucial for predisposing VVD to the dimer state, it does not fully represent the changes that cause light-excited VVD to associate as a dimer.

The observed spontaneous dimerization of the C71V variant is interesting, given that its scattering profile most closely resembles that of the Dark$_{EXT}$ ensemble. A minimization analysis confirms these states to be a combination of Dark$_{EXT}$ and dimer (see Supplementary Fig. 3), whereas Dark$_{COMP}$ cannot adequately reproduce the data measured for the variant. This result suggests that extension of the Ncap region precedes dimer formation.

## The structure of the VVD light-activated dimer

SAXS data were collected 8.8 s after light activation (see Materials and Methods) of VVD-36 in either the Dark$_{COMP}$ or the Dark$_{EXT}$ conformational ensembles to elucidate the form of the VVD light-activated dimer. On this long time scale, equilibrium between monomers and dimers has been reached. Assuming that the light-activated dimer takes the same form

regardless of the initial protein dark state, we can extract its unique scattering profile by minimizing:

$$\chi_\nu^2 = \sum_q \frac{\left(\left(I_{\mathrm{LightCOMP}}(q) - r_1 I_{\mathrm{2PD7}}(q)\right) - c\left(I_{\mathrm{LightEXT}}(q) - r_2 I_{\mathrm{DarkEXT}}(q)\right)\right)^2}{\sigma^2_{\mathrm{LightCOMP}}(q) + \sigma^2_{\mathrm{LightEXT}}(q) + \sigma^2_{\mathrm{DarkEXT}}(q)}$$

Here, $I_x(q)$ are scattering profiles from the different VVD measurements, distinguished by the characteristic scattering of the dark state. For this computation, the scattering profile derived from the 2PD7 structure was employed in place of $\mathrm{Dark_{COMP}}$ to minimize the overall noise. The terms in the denominator represent the errors associated with each measurement. The three parameters $r_1$, $r_2$, and $c$, which account for fractions of unphotolyzed protein present in each sample and variations in protein concentration, were varied to minimize $\chi^2$. The values of $r_1$ and $r_2$ are 0.62 and 0.83, respectively, indicating a mixture of monomer and dimer in each state. Since the dimer fraction varied considerably in the absence of DTT, we hesitate to assign much significance to its absolute value. However, this analysis is valuable because it enables extraction of the scattering profile of the pure light-excited dimer from the data, as $I_{\mathrm{LightCOMP}}(q) - r_1 I_{\mathrm{2PD7}}(q)$ or $c\left(I_{\mathrm{LightEXT}}(q) - r_2 I_{\mathrm{DarkEXT}}(q)\right)$. Reconstruction methods were applied (see below) and yield structural information about the dimer. The close agreement of the dimer scattering profiles obtained from either ensemble (see Supplementary Fig. 4) and the $\chi_\nu^2$ of 0.68 demonstrate the validity of the original assumption. Thus, these four scattering curves can be well described by a model containing only three states. At this resolution, photoactivated VVD forms the same structure regardless of the conformation of the dark state.

Significantly, the robust scattering profile obtained for the VVD dimer does not match the scattering curve calculated from the dimer found in the asymmetric unit of the crystal structure (see Supplementary Fig. 5). This disagreement is not surprising; the crystallized dimer is unlikely to be functionally relevant.[18] Even for photoexcited crystals,[17] the crystal packing interactions likely prevent the full conformational changes needed to gate functional dimerization and surely preclude rearrangement to a different dimer. To investigate the structure of the solution, light-induced dimer, we reconstructed low-resolution molecular envelopes from the scattering profiles of the pure dimer, derived as described above. These methods produced a shape with 2-fold symmetry (Fig. 6), regardless of whether or not the reconstruction program was seeded with this information. In contrast to the cylindrical outline of the crystallographic dimer, this shape has a large bulge along the dyad axis, indicating an expansion of the molecule at the dimer interface and a contraction of the molecule along the long axis perpendicular to the molecular interface. Importantly, we could find no orientation of the crystallographic VVD-36 monomer that upon application of 2-fold symmetry could fit the reconstructed envelope. Thus, the subunit in the light-induced dimer must have a conformation substantially different from that held by the dark-state, crystallographic monomer.

## Discussion

SAXS profiles of light- and dark-adapted states of VVD-36 and a C71V SAXS data are effectively described by linear combinations of scattering profiles from three states: the monomer reported in the dark-state crystal structure, the same monomer with an extended N-terminus, and a light-state dimer composed of subunits with structures that are

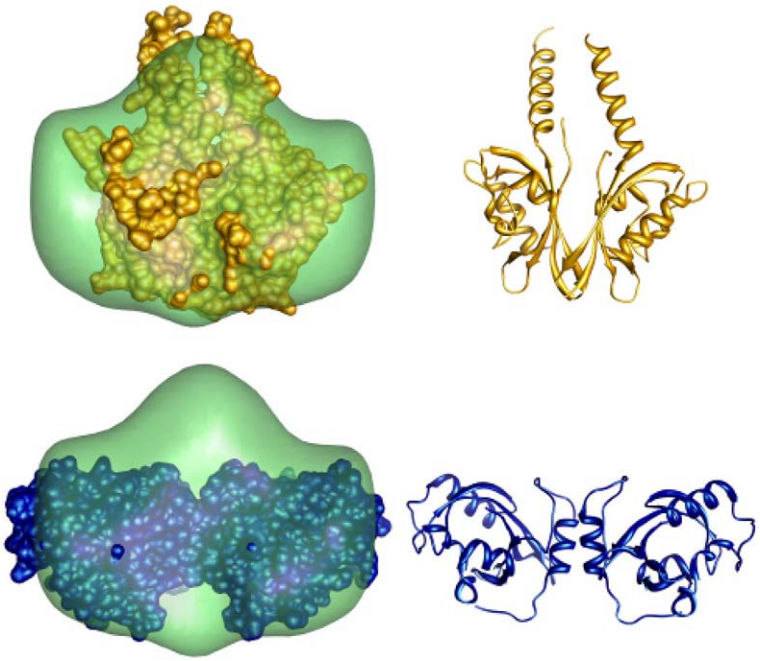

**Fig. 6.** Molecular envelope of the VVD light-activated dimer. The smooth envelope represents a shape reconstruction based on the scattering profile of the dimer, extracted by minimization analysis. The mean normalized spatial discrepancy of the reconstruction is 0.55, indicating a unique envelope shape. The top image also shows the structure of YtvA, a dimeric LOV domain with a very different dimer interface compared to that found in the VVD crystal structure. At left, the two structures are superimposed; the ribbon diagram of YtvA is shown at right. The bottom panel illustrates the superposition of the crystallized VVD dimer on the reconstructed shape. The VVD ribbon diagram is shown at the bottom, right. The reconstructed shape suggests that the VVD solution dimer has extended structure, perhaps with helices similiar to YtvA.

distorted compared to the crystal structure. Furthermore, VVD-36 molecules can become oxidized to a form that chemically resembles the nonfunctional C71S mutant. This evidence raises further questions such as the following: What distinguishes $Dark_{EXT}$ from $Dark_{COMP}$? What is the relationship between $Dark_{EXT}$ and the C71V mutant dark state? How does a unique dimer structure emerge from two distinct starting conformations? Consideration of these points leads us to propose a model for the conformational transitions involved in VVD activation.

As stated above, the C71V variant of VVD partially dimerizes without light, suggesting that its monomer form closely mimics the light-induced conformation that is competent for dimerization. Light excitation results in additional dimerization. In contrast, $Dark_{EXT}$ has the same scattering profile as the variant monomer but does not dimerize until exposure to light. These functional distinctions indicate conformational differences between C71V and $Dark_{EXT}$ beyond the resolution of these ensemble measurements. Modeling demonstrates good, albeit not necessarily unique, agreement between $Dark_{EXT}$ and a system where the ~28 N-terminal amino acids are treated as a flexible ensemble. Involvement of Ncap conformational change in light activation is also supported by (a) the structure of the molecule, which shows the Ncap near the surface and thus extendable; (b) crystal structures, which demonstrate that alternate conformations of the N-terminus are possible; (c) movement of structural elements that stabilize the Ncap against the PAS core in light-excited crystals; (d) residues buried beneath the Ncap that, when altered, affect the dimerization equilibrium; (e) involvement of N-terminal regions in the constitutive dimerization of other PAS domains;[21,27] and (f) subunit cross-linking patterns in the light-induced dimer that are best explained if the N-terminus assumes a different position than it does in the dark-state crystal structure. Taken together, the current data support a structural model in which the Ncap packs weakly against the PAS scaffold, in a manner that allows transient undocking from the PAS core. We propose that this undocking exposes and stabilizes the interaction surface.

Differences in the extent of dimerization in $Dark_{EXT}$ and C71V dark and light states, despite their common scattering states, must result from subtle changes in molecular structure. SAXS is a low-resolution technique; small changes in molecular conformation or shifts in ensemble populations may be imperceptible. While our data are consistent with extensive undocking of the N-terminus, they do not indicate the exact size or orientation of the undocked region; neither do they favor a homogeneous *versus* heterogeneous population of states. Additional conformational or chemical changes to the extended state might shift the orientation or stabilize a subpopulation and alter the dimerization potential, explaining why $Dark_{EXT}$ does not dimerize but C71V (dark) does. The more extensive dimerization of C71V in the light state implies some degree of continuity between these extended states. Mutation of a cysteine to a valine at a key site could limit possible conformations of an otherwise flexible extended state, facilitating formation of a small fraction of dimer in the dark state, while light activation further stabilizes the interface involved in dimer formation. Alternatively or additionally, Cys71 could participate directly in the dimer interface and substitution to Val could stabilize subunit contacts. Either case could account for the dimerization patterns we report here.

Either the extended monomer ($Dark_{EXT}$) or the compact monomer ($Dark_{COMP}$) can dimerize on light excitation, and the structure of the dimer formed is the same in each case (see Fig. 7). Unlike the C71V variant, there is no change in protein sequence that explains the difference between these two populations. However, Cys71 also turns out to be a prominent site of oxidation on the protein in that it forms a sulfenic acid after incubation in aerated buffer. Because oxidation inhibits light-induced dimerization, we must conclude that this modification (S-OH) stabilizes the compact monomer to a degree that disfavors progression to the extended precursor state. This is consistent with the observations that the C71S substitution will also not undergo any light-induced dimerization and that protein oxidation also inhibits dimerization (Supplementary Fig. 1). A Ser substitution at residue 71, like a sulfenic acid, buries a hydrogen-bonding hydroxyl group into the turn that separates the Ncap from the PAS core. In fact, both the sulfenic acid and Ser at position 71 hydrogen bond to the same backbone amide on bβ, which shifts in crystal structures of light-activated VVD-36. We suspect that the hydroxyl-to-amide hydrogen bond present in both C71S and oxidized VVD-36 locks the hinge region in the inactive conformation.

The presence of the two distinct dark states in the VVD-36 population may then be related to oxidation at Cys71, identified above as a key switch point that leads to VVD dimerization. Given that the protein preparations that lead to $Dark_{EXT}$ had minimal oxygen exposure or could be generated by treatment with reductant, $Dark_{EXT}$ likely represents the unoxidized form of the protein. However, since crystal structures of VVD that do not have Cys71 oxidized are composed of compact molecules, we must conclude that crystallization itself stabilizes the N-terminus against the PAS core. (This is not surprising given that the Ncap forms extensive crystal contacts in the lattice.) The increases in $I(0)$ and the fitting constants $r_1$ and $r_2$ give very rough estimates of dimerization and indicate that both populations of molecules dimerize extensively on exposure to light. Mass spectrometry analysis and some high-resolution crystal structures indicate that Met residues also undergo partial oxidation in VVD-36. The extent of oxidation at key residues may provide a biologically relevant mechanism to tune the structure and the extent of dimerization in the same way that mutation of the residues has been observed to affect both (above and Refs. 17

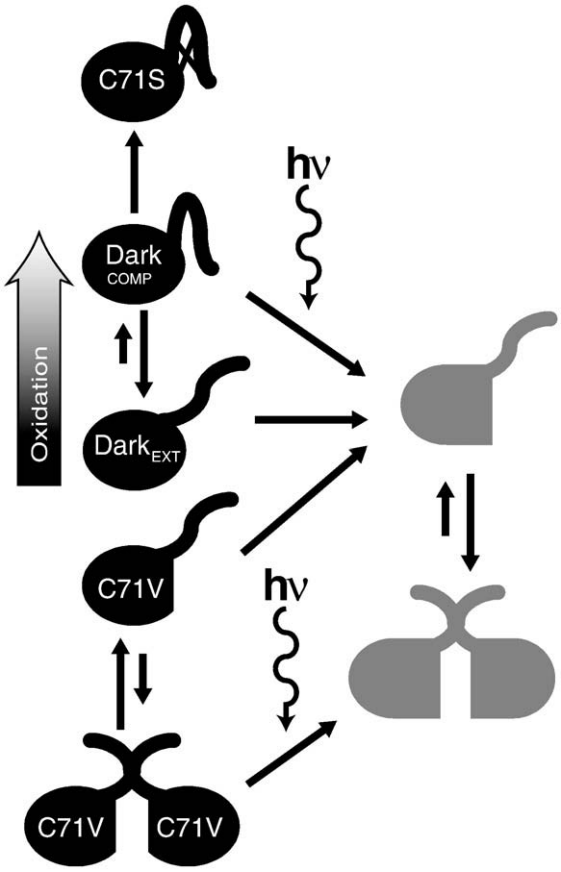


**Fig. 7.** Scheme illustrating the proposed dimerization mechanism. All of the dark states discussed in the text are shown on the left, in a continuum from less (top) to more (bottom) competent for dimerization. In the case of extensive oxidation or mutation of Cys71 to Ser, shown at the top of the left column, the protein does not dimerize. Despite small differences in the structures of the Dark$_{COMP}$ and Dark$_{EXT}$ states, a common dimer forms following illumination. In agreement with reconstructions, the Ncaps detach from the core and extend upwards along the dimer interface in the orientation shown in this scheme. Differences in conformation resulting from mutation of Cys71 to Val appear to be below the resolution of these SAXS experiments but are evidenced by partial VVD dimerization in the absence of light, suggested by the dark-state dimer at the bottom of the left column. Upon light excitation, additional conformational changes enhance the dimer fraction of these proteins as well.

and 18). In fact, it has been demonstrated that under conditions of oxidative stress, *Neurospora* shows behavior consistent with VVD inactivation.[16] Specifically, a mutant in super oxide dismutase, *sod* exhibits increased production of carotenoids following exposure to blue light, which is analogous to the *vvd* null phenotype.[16] Moreover, the response to reactive oxygen species is enhanced in the *sod: vvd* double mutant. Upregulation of carotenoid biosynthesis through *vvd* inactivation may be an effective strategy for scavenging radicals and preventing damage under conditions of oxidative stress.

Whether or not the two VVD dark states are represented *in vivo*, they provide insight into the conformational processes that gate and mediate light-induced dimerization of VVD. Adoption of the extended state is necessary, but not sufficient, for subunit association, and factors that favor the compact state, for example, oxidation, inhibit subunit association. The compact state is well represented by the previously determined crystal structure, and it would be difficult to imagine that the specific contacts made by the Ncap were not relevant for the fold of the protein in some context. These properties then provide physicochemical constraints upon which biological function can be based. In the context of full-length VVD within the cell and surrounded by potential partners, the protein may primarily assume a compact form. Regardless, upon light activation, the protein must transition through an extended state prior to dimerization. The expanded dark state is newly characterized here as a feature of the conformational switches that ultimately produce light-induced dimerization.

In spite of the distinct states present in dark-adapted VVD, a common structure for the light-activated dimer is measured. Reconstruction of the dimer curve supports conclusions from previous work that the solution dimer takes a different form from the crystallized dimer.[18] This is not surprising, given that the crystal structure was obtained by light exposure of a crystal containing dark-adapted VVD that has already formed a dimer. The reconstructed envelope depicts a dimer with a single bulge on the dyad axis, which we speculate is due to the rearranged Ncaps of both molecules. The molecular envelope suggests that the dimer is parallel with respect to the orientation of the central β-scaffold, an orientation consistently present in homodimeric PAS dimers.[21,27–29] Such a model is suggestive of the related bacterial LOV domain YtvA,[20] which displays a dimer interface between β-sheets, with no appreciable intervening Ncap. Instead, a C-terminal helix extends up along the dimer plane, producing a shape similar to our reconstructed envelope. Parallel orientations are also found in homodimers of Arnt and HIF[30] and those of the LOV1 and LOV2 subdomains from phototropins.[24,28,31] However, we note that the ARNT:HIF heterodimers are antiparallel with respect to the β-strand directions. Adopting a parallel arrangement in VVD would place the loops containing residue 171 in close contact, consistent with observed light-induced solution cross-linking from residues at that position.[18] A number of different arrangements are known for PAS dimers associated through the subunit β-sheets, although the same residue positions often participate in the respective interfaces.[32] In VVD, these conserved contact sites generally hold hydrophobic residues that could also mediate dimerization.

VVD has been shown to work in concert with WC-1 to regulate circadian rhythms in *N. crassa*.[12] Indeed, VVD antagonizes the ability of WC-1 to activate gene transcription in response to light and thus generates an adaptive response. The mecha-

nism for this signaling pathway has yet to be determined. Transient dimerization coupled to conformational dynamics in PAS domains has been observed in phototropins[24,33–36] and HIF:ARNT heterodimers.[23,30] In phototropins, N-terminal and C-terminal elements similar to the VVD N-terminal α-helix have been shown to undergo large-scale conformational changes following photoexcitation.[23,30] The HIF:ARNT system is intriguing in its similarities. In this case, the HIF:ARNT heterodimer competes with the ARNT homodimer on the signaling pathway.[23,30] Notably, WC-1 has a very similar LOV domain to VVD and perhaps both homo- and heterodimerization of these domains are important elements in their regulation.[18]

In conclusion, the combined data present a model in which light-driven flavin adduct chemistry in VVD reorganizes structural elements adjacent to the β-scaffold. The reorganized surface is then conducive to subunit association. Such a system is highly adaptive because evolution can remodel the mobile elements to incorporate different effector modules and the interaction surface to target different partners. For example, phototropin LOV domains display a similar mechanism but recruit a C-terminal helix as the mobile elements instead of the Ncap.[37] The degree to which the signaling processes of LOV/PAS domains are similar or divergent likely forms a continuum, which is only beginning to be described. Visualization of transient states via SAXS reconstructions has the potential to elucidate key aspects of these mechanisms and thereby broaden our understanding of how proteins transduce environmental stimuli into cellular responses.

## Materials and Methods

### Sample preparation

#### *Preparation of VVD variants*

The C71V variant of VVD-36 was produced and characterized in a previous study.[18] However, to help ward against the complicating issues associated with oxidation and protein instability, we produced this variant in the background of C183S, which has a known site of oxidation (Cys183) removed. The C71V:C183S variant was constructed according to the QuikChange protocol (Stratagene). Resultant mutants were sequenced in their entirety at the Biotechnology Resource Center at Cornell University.

#### *Protein expression and purification*

VVD-36 and C71V:C183S variants were overexpressed in *Escherichia coli* BL21(DE3) cells. Two-liter cultures of the variants were grown to an $OD_{600}$ (optical density at 600 nm) of 0.6–0.8 at 37 °C. When the cell density reached 0.6, the cultures were cooled to 18 °C and induced with 100 M IPTG. Protein was then expressed for 22 h prior to harvesting the cells.

Twenty-four liters of both VVD-36 and C71V:C183S were prepared via the above protocol and lysed in buffer containing 13% glycerol, 300 mM NaCl, 50 mM Hepes, pH 8.0, and 5 mM imidazole, pH 8; the sonicated and soluble cell lysate was fractionated by centrifugation. The supernatant was then collected and protein purified via Ni:NTA affinity chromatography. Eluted VVD was subsequently treated with 1 unit of thrombin per milligram of protein for 6 h in buffer containing 2 mM DTT, 13% glycerol, 150 mM NaCl, 50 mM Hepes, pH 8.0, and 100 mM imidazole. The protein was then purified on a Superdex 75 26/60 Hi-load column and concentrated to 5 mg/mL. Final protein samples contained 5 mM DTT.

#### *Crystallization of oxidized VVD*

VVD-36 was cocrystallized in the presence of 10 mM imidazole via the hanging drop method. Crystals grew from droplets containing 2 μl each of 5 mg/ml VVD-36 and 2 μl of the reservoir solution containing 20 mM imidazole, 100 mM NaCl, 26% polyethylene glycol 4000, and 100 mM trisodium citrate, pH 5.6. Crystals were obtained overnight at 22 °C and diffracted to 2.3 Å resolution at the F3 beamline at the Cornell High Energy Synchrotron Source (CHESS). Diffraction data for 30–2.3 Å was processed with HKL2000, and the structure was determined using molecular replacement (AMORE) using 2PD7 as a search model. The model was rebuilt using Xfit followed by positional and thermal refinement in CNS. Residual density in $2F_o-F_c$ (2 σ) and $F_o-F_c$ (3 σ) connecting to the Cys71 side chain was consistent with oxidation to cysteinic acid (Cys-OH).

### SAXS data collection

SAXS data were collected at the G1 beamline at the CHESS at an energy of 8 keV. A continuous flow cell made of a 1-mm polyester tube (Advanced Polymers, Inc., VT)[38] was employed to collect time-resolved data, using a method described in Ref. 18. A 473-nm laser from Holograms and Laser, International (Houston, TX) was aligned with the X-ray beam using a 20-μm slit to confirm their coincidence. The X-ray beam was focused with a glass capillary[39,40] for better position definition. The laser focal point was then moved against the direction of fluid flow to introduce delay. Eight 30-s X-ray exposures were collected on the protein for each sample, to improve signal to noise and ensure reproducibility. A PIN diode was mounted onto the X-ray beamstop to measure changes in beam intensity.

Although this method allows for data to be collected at several points after light excitation, minimal changes were observed after the first data point (Supplementary Figs. 6 and 7 and Supplementary Discussion). Previous time-resolved SAXS measurements on VVD reflected additional conformational changes after several seconds, in contrast to current observations.[19] The main difference between these measurements was the current inclusion of DTT in the protein buffer. This may indicate that oxidation is associated with conformational changes in the light-excited state. Static SAXS experiments confirm that synchrotron X-ray exposure reduces the VVD flavin and thereby inhibit dimerization.[17] However, the flow cell configuration greatly diminishes X-ray exposure and thereby mitigates problems associated with flavin reduction. In flow cell experiments, the X-ray exposure time was varied simply by changing the flow speed (while carefully ensuring identical light exposure of the sample). No effect on the yield of VVD dimerization with X-ray exposure was found. UV/Vis absorption spectra collected on samples after irradiation and X-ray exposure confirmed a substantial conversion of VVD to the light-state adduct.

### Data analysis

Images were converted to scattering profiles of intensity ($I$) as a function of $q$, where $q = \frac{4\pi\sin\theta}{\lambda}$, with θ being half the scattering angle and λ being the X-ray wavelength. An image of a silver stearate[41] scattering ring collected under the same beam conditions was used to find the beam center and determine the radial calibration. Each scattering profile was normalized for changes in beam intensity and checked for reproducibility. Final scattering profiles were obtained using MATLAB (The Mathworks, Natick, MA) by first averaging images and then converting the data to intensity *versus* $q$ and subtracting the buffer background.

Scattering data plotted as a Guinier plot, $\log(I(q))$ *versus* $q^2$, is approximately linear at low angles.[42] Typically, this approximation is considered valid for $qR_g<1.3$. Fitting to this line allows extrapolation to $I(0)$ and provides the slope, which is proportional to $R_g$. Errors on these quantities were determined by propagating the 95% confidence intervals from the slope and $y$-intercept of the line fit with MATLAB.

GNOM, DAMMIN, DAMAVER, CRYSOL, and EOM are all analysis tools for scattering data made available by the Biological Small Angle Scattering group at the European Molecular Biology Laboratory.[43] CRYSOL was used to calculate scattering from crystal structures. Scaling was determined by CRYSOL through comparison to appropriate experimental data. Conversion of scattering data to $P(r)$ was done with GNOM.[44] In general, $D_{max}$ was found by testing input values to GNOM based on the $R_g$ determined from Guinier analysis and choosing the one which best maximized the default regularization parameters used by GNOM. We determined $D_{max}$ to within 5 Å with this method.

All minimizations described in the text were performed using the fmin function in MATLAB. Statistical errors for the analysis were determined using GNOM based on the noise in the data. Degrees of freedom, $v$, were calculated by subtracting the number of fitting parameters from the number of points in a single scattering curve. Reconstructions were carried out by running DAMMIN[45] 10 times on the output from GNOM and then using DAMAVER to average the results and Situs[46] to generate a shape envelope. Crystal structures were fitted in the molecular envelopes also using Situs. Analysis with EOM was carried out using the 3D72 crystal structure. Data for the Cys71 sulfenic acid form of Vivid have been deposited with the RCSB Protein Data Bank with PDB ID code 3IS2.

## Acknowledgements

Funding for this work was provided by the Cornell Nanobiotechnology Center, which is supported by the STC Program of the National Science Foundation under Agreement No. ECS-9876771. This work was also supported by National Institutes of Health grant R01-GM079679. CHESS is supported by the National Science Foundation and the National Institutes of Health/National Institute of General Medical Sciences under award DMR-0225180. The authors would like to thank Sterling Cornaby and Arthur Woll for their assistance at the G1 station and Steve Meisburger for valuable comments. Computations were carried out at the Cornell Center for Materials Research.

## Supplementary Data

Supplementary data associated with this article can be found, in the online version, at doi:10.1016/j.jmb.2009.08.045

## References

1. Pellequer, J. L., Wager-Smith, K. A., Kay, S. A. & Getzoff, E. D. (1998). Photoactive yellow protein: a structural prototype for the three-dimensional fold of the PAS domain superfamily. *Proc. Natl Acad. Sci. USA*, **95**, 5884–5890.
2. Taylor, B. L. & Zhulin, I. B. (1999). PAS domains: internal sensors of oxygen, redox potential, and light. *Microbiol. Mol. Biol. Rev.* **63**, 479–506.
3. Swartz, T. E., Corchnoy, S. B., Christie, J. M., Lewis, J. W., Szundi, I., Briggs, W. R. & Bogomolni, R. A. (2001). The photocycle of a flavin-binding domain of the blue light photoreceptor phototropin. *J. Biol. Chem.* **276**, 36493–36500.
4. Briggs, W. R., Christie, J. M. & Salomon, M. (2001). Phototropins: a new family of flavin-binding blue light receptors in plants. *Antioxid. Redox Signal.* **3**, 775–788.
5. Crosson, S., Rajagopal, S. & Moffat, K. (2003). The LOV domain family: photoresponsive signaling modules coupled to diverse output domains. *Biochemistry*, **42**, 2–10.
6. Losi, A. (2004). The bacterial counterparts of plant phototropins. *Photochem. Photobiol. Sci.* **3**, 566–574.
7. Salomon, M., Eisenreich, W., Durr, H., Schleicher, E., Knieb, E., Massey, V. *et al.* (2001). An optomechanical transducer in the blue light receptor phototropin from *Avena sativa*. *Proc. Natl Acad. Sci. USA*, **98**, 12357–12361.
8. Crosson, S. & Moffat, K. (2002). Photoexcited structure of a plant photoreceptor domain reveals a light-driven molecular switch. *Plant Cell*, **14**, 1067–1075.
9. Huala, E. (1997). Arabidopsis NPH1: a protein kinase with a putative redox-sensing domain. *Science*, **278**, 2120–2123.
10. Crosson, S. & Moffat, K. (2001). Structure of a flavin-binding plant photoreceptor domain: insights into light-mediated signal transduction. *Proc. Natl Acad. Sci. USA*, **98**, 2995–3000.
11. Loros, J. J. & Dunlap, J. C. (2001). Genetic and molecular analysis of circadian rhythms in *Neurospora*. *Annu. Rev. Physiol.* **63**, 757–794.
12. Brunner, M. & Kaldi, K. (2008). Interlocked feedback loops of the circadian clock of *Neurospora crassa*. *Mol. Microbiol.* **68**, 255–262.
13. Ávila-Pérez, M., Hellingwerf, K. J. & Kort, R (2006). Blue light activates the $\sigma^B$-dependent stress response of *Bacillus subtilis* via YtvA. *J. Bacteriol.* **188**, 6411–6414.
14. Heintzen, C., Loros, J. J. & Dunlap, J. C. (2001). The PAS protein VIVID defines a clock-associated feedback loop that represses light input, modulates gating, and regulates clock resetting. *Cell*, **104**, 453–464.
15. Schwerdtfeger, C. & Linden, H. (2001). Blue light adaptation and desensitization of light signal transduction in *Neurospora crassa*. *Mol. Microbiol.* **39**, 1080–1087.

16. Yoshida, Y. & Hasunuma, K. (2004). Reactive oxygen species affect photomorphogenesis in *Neurospora crassa*. *J. Biol. Chem.* **279**, 6986–6993.
17. Zoltowski, B. D., Schwerdtfeger, C., Widom, J., Loros, J. J., Bilwes, A. M., Dunlap, J. C. & Crane, B. R. (2007). Conformational switching in the fungal light sensor vivid. *Science*, **316**, 1054–1057.
18. Zoltowski, B. D. & Crane, B. R. (2008). Light activation of the LOV protein Vivid generates a rapidly exchanging dimer. *Biochemistry*, **47**, 7012–7019.
19. Lamb, J. S., Zoltowski, B. D., Pabit, S. A., Crane, B. R. & Pollack, L. (2008). Time-resolved dimerization of a PAS-LOV protein measured with photocoupled small angle X-ray scattering. *J. Am. Chem. Soc.* **130**, 12226–12227.
20. Möglich, A. & Moffat, K. (2007). Structural basis for light-dependent signaling in the dimeric LOV domain of the photosensor YtvA. *J. Mol. Biol.* **373**, 112–126.
21. Ma, X. L., Sayed, N., Baskaran, P., Beuve, A. & van den Akker, F. (2008). PAS-mediated dimerization of soluble guanylyl cyclase revealed by signal transduction histidine kinase domain crystal structure. *J. Biol. Chem.* **283**, 1167–1178.
22. Strickland, D., Moffat, K. & Sosnick, T. R. (2008). Light-activated DNA binding in a designed allosteric protein. *Proc. Natl Acad. Sci. USA*, **105**, 10709–10714.
23. Card, P. B., Erbel, P. J. A. & Gardner, K. H. (2005). Structural basis of ARNT PAS-B dimerization: use of a common beta-sheet interface for hetero- and homodimerization. *J. Mol. Biol.* **353**, 664–677.
24. Nakasone, Y., Eitoku, T., Matsuoka, D., Tokutomi, S. & Terazima, M. (2006). Kinetic measurement of transient dimerization and dissociation reactions of *Arabidopsis* phototropin 1 LOV2 domain. *Biophys. J.* **91**, 645–653.
25. Nakasako, M., Iwata, T., Matsuoka, D. & Tokutomi, S. (2004). Light-induced structural changes of LOV domain-containing polypeptides from *Arabidopsis* phototropin 1 and 2 studied by small-angle X-ray scattering. *Biochemistry*, **43**, 14881–14890.
26. Bernadó, P., Pérez, Y., Svergun, D. I. & Pons, M. (2008). Structural characterization of the active and inactive states of Src kinase in solution by small-angle X-ray scattering. *J. Mol. Biol.* **376**, 492–505.
27. Key, J., Hefti, M., Purcell, E. B. & Moffat, K. (2007). Structure of the redox sensor domain of *Azotobacter vinelandii* NifL at atomic resolution: signaling, dimerization, and mechanism. *Biochemistry*, **46**, 3614–3623.
28. Nakasako, M., Zikihara, K., Matsuoka, D., Katsura, H. & Tokutomi, S. (2008). Structural basis of the LOV1 dimerization of *Arabidopsis* phototropins 1 and 2. *J. Mol. Biol.* **381**, 718–733.
29. Lee, J., Tomchick, D. R., Brautigam, C. A., Machium, M., Kort, R., Hellingwerf, K. J. & Gardner, K. H. (2008). Changes at the KinA PAS-A dimerization interface influence histidine kinase function. *Biochemistry*, **47**, 4051–4064.
30. Erbel, P. J. A., Card, P. B., Karakuzu, O., Bruick, R. K. & Gardner, K. H. (2003). Structural basis for PAS domain heterodimerization in the basic helix–loop–helix PAS transcription factor hypoxia-inducible factor. *Proc. Natl Acad. Sci. USA*, **100**, 15504–15509.
31. Salomon, M., Lempert, U. & Rudiger, W. (2004). Dimerization of the plant photoreceptor phototropin is probably mediated by the LOV1 domain. *FEBS Lett.* **572**, 8–10.
32. Ayers, R. A. & Moffat, K. (2008). Changes in quaternary structure in the signaling mechanisms of PAS domains. *Biochemistry*, **47**, 12078–12086.
33. Harper, S. M., Neil, L. C. & Gardner, K. H. (2003). Structural basis of a phototropin light switch. *Science*, **301**, 1541–1544.
34. Harper, S. M., Neil, L. C., Day, I. J., Hore, P. J. & Gardner, K. H. (2004). Conformational changes in a photosensory LOV domain monitored by time-resolved NMR spectroscopy. *J. Am. Chem. Soc.* **126**, 3390–3391.
35. Nakasone, Y., Eitoku, T., Matsuoka, D., Tokutomi, S. & Terazima, M. (2007). Dynamics of conformational changes of *Arabidopsis* phototropin 1 LOV2 with the linker domain. *J. Mol. Biol.* **367**, 432–442.
36. Nakasone, Y., Ono, T. A., Ishii, A., Masuda, S. & Terazima, M. (2007). Transient dimerization and conformational change of a BLUF protein: YcgF. *J. Am. Chem. Soc.* **129**, 7028–7035.
37. Ko, W. H., Nash, A. I. & Gardner, K. H. (2007). A LOVely view of blue light photosensing. *Nat. Chem. Biol.* **3**, 372–374.
38. Kalinin, Y., Kmetko, J., Bartnik, A., Stewart, A., Gillilan, R., Lobkovsky, E. & Thorne, R. (2005). A new sample mounting technique for room-temperature macromolecular crystallography. *J. Appl. Crystallogr.* **38**, 333–339.
39. Engström, P., Larsson, S., Rindby, A., Buttkewitz, A., Garbe, S., Gaul, G. *et al.* (1991). A submicron synchrotron X-ray beam generated by capillary optics. *Nucl. Instrum. Methods Phys. Res., Sect. A*, **302**, 547–552.
40. Lamb, J. S., Cornaby, S., Andresen, K., Kwok, L., Park, H. Y., Qiu, X. *et al.* (2007). Focusing capillary optics for use in solution small-angle X-ray scattering. *J. Appl. Crystallogr.* **40**, 193–195.
41. Vand, V., Aitken, A. & Campbell, R. K. (1949). Crystal structure of silver salts of fatty acids. *Acta Crystallogr.* **2**, 398–403.
42. Guinier, A. & Fournet, G. (1955). *Small-Angle Scattering of X-Rays.* John Wiley and Sons, New York, NY.
43. Konarev, P. V., Petoukhov, M. V., Volkov, V. V. & Svergun, D. I. (2006). ATSAS 2.1, a program package for small-angle scattering data analysis. *J. Appl. Crystallogr.*, 277–286.
44. Svergun, D. I. (1992). Determination of the regularization parameter in indirect-transform methods using perceptual criteria. *J. Appl. Crystallogr.* **25**, 495–503.
45. Svergun, D. I. (1999). Restoring low resolution structure of biological macromolecules from solution scattering using simulated annealing. *Biophys. J.* **76**, 2879–2886.
46. Wriggers, W. & Chacón, P. (2001). Using Situs for the registration of protein structures with low-resolution bead models from X-ray solution scattering. *J. Appl. Crystallogr.* **34**, 773–776.